Dynamic Centrifuge Modeling of Sound Walls Supported on Concrete Cantilever and Mechanically Stabilized Earth Retaining Structures

DAVID SOON, JOHN A. CASEY, BRUCE L. KUTTER, AND KARL M. ROMSTAD

The results of a model study comparing the dynamic behavior of sound walls supported on concrete cantilever (Caltrans Standard Type 1) and mechanically stabilized earth (MSE) retaining structures are presented. Different backfills representing a loose sand, a dense sand, and a cohesive material were studied. An additional test was run with the loose sand and inclined reinforcing. The models were tested on a servohydraulic shaking table mounted on a centrifuge. Realistic earthquakes with peak input base accelerations of 0.65 *g* to 0.75 *g* were simulated. The sound wall response on the MSE system involved accumulated tilting due to nonsymmetrical resistance, and in some cases lift-off and impact of the slab. The behavior of sound walls on Type 1 systems was much less sensitive to the backfill type. The MSE systems were generally more ductile than the Type 1 walls; they suffered larger permanent deformations but transmitted smaller accelerations to the sound wall. Sound wall accelerations on the Type 1 wall system were approximately twice those on the MSE system.

Mechanically stabilized earth (MSE) retaining systems are often cost-effective alternatives to conventional retaining walls. However, in areas of significant seismic activity, the dynamic behavior of sound walls superimposed on MSE systems is unknown, and design engineers have been reluctant to use systems for which there is little field or experimental data. Because of this lack of data and the policy of the California Department of Transportation (Caltrans) to encourage the use of alternative retaining systems, this research project was initiated.

Kutter, in another paper in this Record, presents a discussion of scaling laws and the advantages and disadvantages of dynamic centrifuge modeling. The disadvantages become less critical if a modeler uses the centrifuge as a tool to compare the performance of different types of structures while the grain size, boundary conditions, and loading rates are held constant. This paper presents such a study in which MSE walls are compared with conventional reinforced concrete cantilever (Type 1) retaining walls.

The models tested in this study represented 24-ft-high prototype earth retaining structures with 12-ft sound walls positioned on top of the retaining structures. The models represented a typical reinforced concrete cantilever retaining wall called a Type 1 retaining wall by Caltrans. Figure 1a shows a schematic of the prototype Type 1 retaining wall system. The system includes a vehicle barrier and a roadway slab in addition to the reinforced masonry block sound wall. The sound wall is anchored directly to the reinforcing bars of the Type 1 retaining wall, creating a continuous structure.

The alternative soil retaining structure tested is a reinforced soil wall that Caltrans calls an MSE wall. Figure 1b is a schematic of the prototype MSE retaining wall. In this wall arrangement the vehicle barrier and sound wall are mounted on the roadway slab, which is anchored to the backfill by short piles. The MSE face plates, which serve to retain the adjacent soil, are held in place by bar mat reinforcing mesh. The reinforcing mesh (bar mat) for this prototype is made of welded rebar.

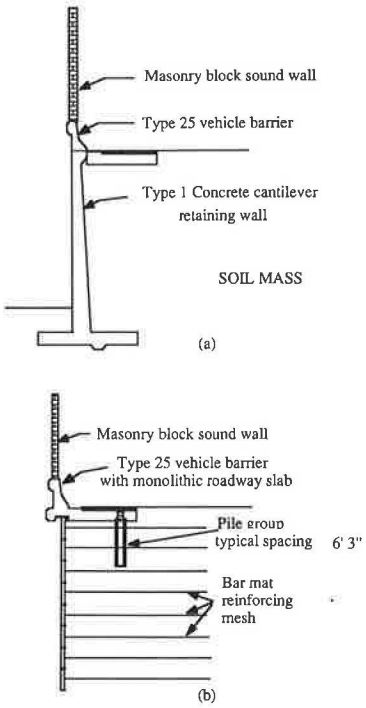

FIGURE 1 ***a*, Type 1 retaining wall; *b*, MSE retaining wall.**

Department of Civil Engineering, University of California, Davis, Calif. 95616.

PREVIOUS RESEARCH

Mononobe and Matsuo (*1*) suggested using the Coulomb sliding wedge theory, with the addition of a lateral acceleration, to predict the resultant lateral force on a gravity retaining wall subjected to an earthquake. The resultant force, which included both static and dynamic pressure, was assumed to act at $\frac{1}{3}H$ above the base. Seed and Whitman (*2*) later recommended that the dynamic component of the pressure resultant should be assumed to act at $0.6H$ above the base. Richards and Elms (*3*) suggested that permanent deformation rather than maximum pressures should be the design criterion. They applied Newmark's sliding block analysis (*4*) to predict wall movement. Bracegirdle (*5*) suggested a limit equilibrium method using a pseudolateral acceleration.

Bolton and Steedman (*6*) and Ortiz et al. (*7*) have conducted centrifuge experiments on cantilever retaining walls supporting dry cohesionless sands subjected to base motions. Richardson and Lee (*8*), Nagel (*9*), and Wolfe and Rea (*10*) have conducted 1-*g* shaking table tests on the seismic behavior of soil-reinforced walls. Later, Richardson (*11*) conducted a field study on a full-scale 20-ft wall to assess his earlier proposed design procedure. Kutter et al. (*12*) and Casey et al. (*13*) have presented preliminary results from this research, field data from earthquakes, and some simple analytical modeling of MSE and Type 1 systems with and without sound walls.

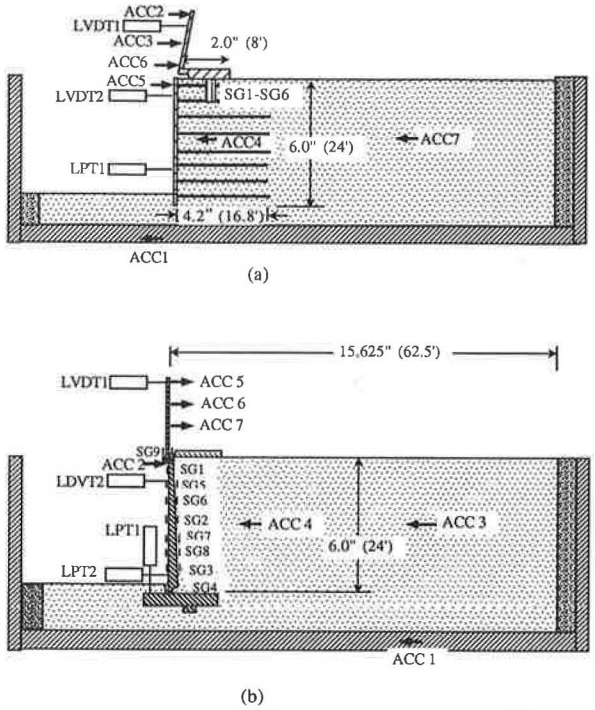

FIGURE 2 Test arrangement and instrumentation: *a*, MSE and *b*, Type 1 retaining wall models.

MODEL RETAINING WALL SYSTEMS

Model Components and Instrumentation

Figure 2a shows the general arrangement and dimensions of the MSE models. Prototype dimensions in Figure 2 are given in parentheses. A coarse wire screen was used to simulate the MSE reinforcing mats which, in the prototype, consist of a mesh of #4 rebar extending 16.8 ft (4.2 in. in model) horizontally into the soil at a vertical spacing of 3 ft (0.75 in. in the model). The total area of the longitudinal reinforcing bars was accurately scaled to that for the prototype. In the prototype MSE design, each 14.5-ft by 3-ft by 8-in.-thick concrete face plate is supported by four mats, each consisting of five 16.8-ft bars (perpendicular to the wall face) spaced at 6 in. with 2-ft-long bars spaced at 18 in. welded across the long bars. In the model, the wire screens were attached to aluminum face plates, which were scaled to simulate the mass of the prototype face plates.

In Figure 2a it can be seen that the sound wall in the model MSE system is tilted at a 9-degree angle to the vertical. This was done to ensure that the radial centripetal acceleration was acting parallel to the wall. The radial acceleration has a lateral component that, for a vertical model wall, would cause an unwarranted static overturning moment. Overturning during the seismic event is a critical failure mechanism for the sound wall of the MSE system.

Figure 2a shows seven accelerometers and three displacement transducers used to measure horizontal accelerations on the sound wall, in the backfill, at the base, and at the top face plate and horizontal deflections at the top of the sound wall, the top face plate, and the third face plate from the bottom. The MSE model system is three face plates wide (across the width of the box) and eight face plates high. The prototype roadway slab (Figure 1b) has a groove that the top face plate fits into without any connection. In preliminary model tests with this arrangement, the accelerations measured at the top face plate showed signs that the top face plate and the sound wall–slab system were making contact. Impact between the sound wall and the top face plate can cause excessively high bar mat forces and local face plate damage. To remedy this problem in later tests the model sound wall system was placed 1 ft (0.25 in. the model) behind the top face plate.

The Type 1 retaining wall model is shown in Figure 2b. The model retaining wall was machined from a solid block of aluminum. The thickness of the Type 1 model was selected to match the computed stiffness of the full-scale concrete cantilever retaining walls; the mass of the concrete wall was not scaled (most of the mass contributing to dynamic loads was assumed to come from the backfill). Because of the rigid connection between the sound wall and the retaining wall in the Type 1 system, it was not considered important to tilt the sound wall. The thickness of the model sound wall was determined by matching its scaled natural frequency to a calculated natural frequency of the prototype 8-in.-thick reinforced masonry block sound wall.

The aluminum model wall (with thickness determined by stiffness criteria) had a higher scaled bending strength than the prototype Type I system. A notch was machined at the base of the aluminum wall to provide the correctly scaled moment capacity at the critical section. Since the notch was relatively short in length, it did not significantly affect the stiffness. The base (13.25-ft prototype) and key dimensions were scaled from the prototype wall with material density

differences (aluminum model versus reinforced concrete prototype) being considered.

Figure 2b shows the location of the strain gauges, displacement transducers, and accelerometers used in the Type 1 models. The Type 1 models were instrumented with nine strain gauges to measure moments in the wall, four displacement transducers to measure deflections, and seven accelerometers to measure accelerations. Only 16 of the instruments could be monitored at once, so each model was tested with three different instrumentation combinations, each involving 16 instruments.

The roadway slabs in both systems were modeled by aluminum plates. The plates represented the mass of a 20-in.-thick concrete slab (8 ft wide) that is used in the roadway shoulder of the prototype system. In the MSE system the slab is anchored to the soil by 6-ft-long, 16-in.-diameter cast-in-place piles spaced at 6.25 ft. These piles were included in the model.

Backfill Conditions Studied

Three backfill soil conditions (denoted as loose, dense, and cohesive) were modeled. The loose backfill was Nevada sand, a fine uniform silica sand with a mean grain size of 0.15 mm and a coefficient of uniformity of 1.7. The loose model was made by spooning the sand into the box layer by layer and vibrating on a vibrating table to achieve the specified density. As commonly specified for prototype walls by Caltrans, the backfill was densified to approximately 93 percent relative compaction California Test #216 compaction test. Because of the poor compaction characteristics of this sand, however, the relative density was only 32 percent. This very loose material had a low friction angle (ϕ = 30 degrees) and no cohesion. The loose backfill is an extreme condition that will tend to show worst-case scenarios for displacements.

The dense backfill soil was also Nevada sand, but the sand was pluviated to obtain a higher density of 101 pcf, relative density of 95 to 100 percent, and a friction angle of 45 degrees. The cohesive backfill consisted of 70 percent Nevada sand with 30 percent Yolo loam (a low-plasticity silty clay). The cohesive backfill was compacted at 12 percent water content by hand to obtain the desired density. The cohesive backfill had a friction angle of 34 degrees, cohesion of 500 psf, density of 103 pcf, and a relative compaction of 92 percent.

One other backfill condition, called loose-10°, was tested for the MSE system. For these tests, the barmats were inclined at a 10-degree angle downward into the backfill.

EXPERIMENTAL PROCEDURE

The shaker, described briefly by Kutter in another paper in this Record, has a sample container that is 11 in. by 22 in. in area and 7 in. in height. A detailed description of the centrifuge system is given by Chang (*14*).

Two prototype acceleration records were used to generate seven types of earthquakes. The records used were from the San Fernando (8244 Orion Blvd., 1st floor, February 9, 1971, 6:00 a.m. PST, North 00° West) and El Centro (Imperial Valley Irrigation District, May 18, 1940, 8:37 p.m. PST, South 00° East) earthquakes. Since the San Fernando record was taken inside a building, the acceleration history includes the soil-structure interactions felt at the first floor of the building. The original El Centro record, in comparison, shows free field response. The alluvial characteristics of the sites at which the accelerations were measured were chosen to match the characteristics of the Harbor Freeway construction area in Los Angeles (deep deposits of firm sandy silt, with approximate standard penetration values of 30 blows per foot).

Two typical achieved acceleration records are shown in Figures 3a and 3b. Note the extended strong motion phase of the record in the San Fernando event of Figure 3a. The strong motion phase of the original record was spliced and reattached to the end to create a long (greater than 30 sec in the prototype) duration of relatively large amplitude accelerations. The prototype acceleration records were processed by double integration, filters, and baseline corrections to create an input data file for the centrifuge shaker. These records could be multiplied by a magnification factor to provide different levels of shaking to the centrifuge models.

Figure 4 shows a comparison of the Caltrans ARS design spectra with the two output spectra from the time histories shown in Figures 3a and 3b. These spectra demonstrate that the models have been subjected to realistic earthquake records. Figure 5a shows the 2 percent damped acceleration response spectra computed using the measured base accelerations for each of the four MSE model types when subjected to the filtered El Centro motion magnified by five. The shape of each of the spectra are similar and the loose-10° and dense models appear to be receiving slightly more energy over most

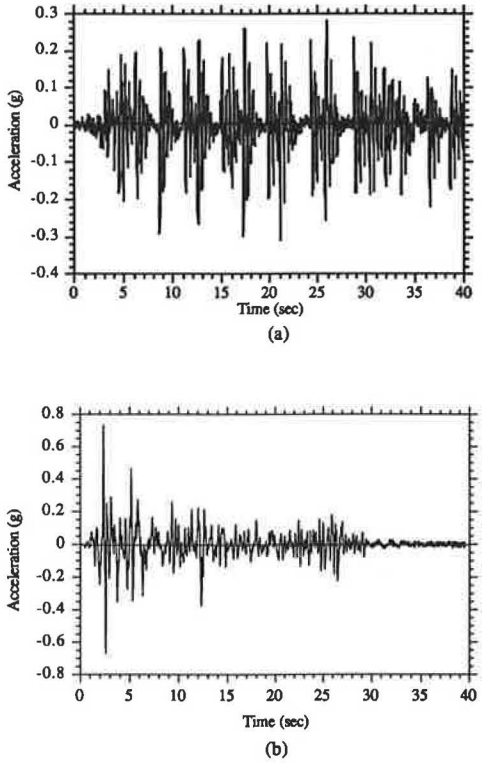

FIGURE 3 Typical achieved base acceleration: *a*, San Fernando × 4 event and *b*, filtered El Centro × 5 event.

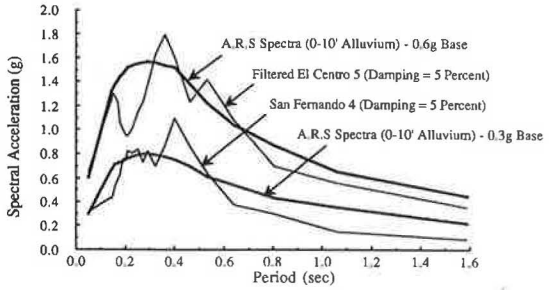

FIGURE 4 Comparison of Caltrans ARS spectral design curves and spectral accelerations from achieved base motions.

of the frequency range. The good repeatability of the base motions allows direct comparison of results. Figure 5b shows that the acceleration response spectra for the base motion during a filtered El Centro event for the Type 1 models was very similar for all three backfill types.

Six models were tested using the Type 1 retaining wall as the soil retaining structure. Four models used the loose sand, one the dense sand, and one had a cohesive backfill. A total of nine models of the MSE retaining wall were tested. Five models used the loose sand, two the dense sand, one the cohesive backfill, and one the loose sand inclined bar mats (loose-10°).

The Type 1 retaining wall systems were subjected to a total of 69 earthquakes, and the MSE retaining wall systems were subjected to 67 earthquakes. For the models used for the comparisons, the typical earthquake sequence of the first six events was (*a*) filtered El Centro × 4 (FEC × 4), (*b*) El Centro × 2 (EC × 2), (*c*) old San Fernando × 4 (OSF × 4), (*d*) filtered El Centro × 5 (FEC × 5), (*e*) El Centro × 4 (EC × 4), and (*f*) new San Fernando × 2 (NSF × 2). The adjectives filtered, old, and new refer to different schemes used for processing the accelerations recorded in the field. Each of these events had a different input base motion. The numbers in the list are an indicator of the intensity of the events.

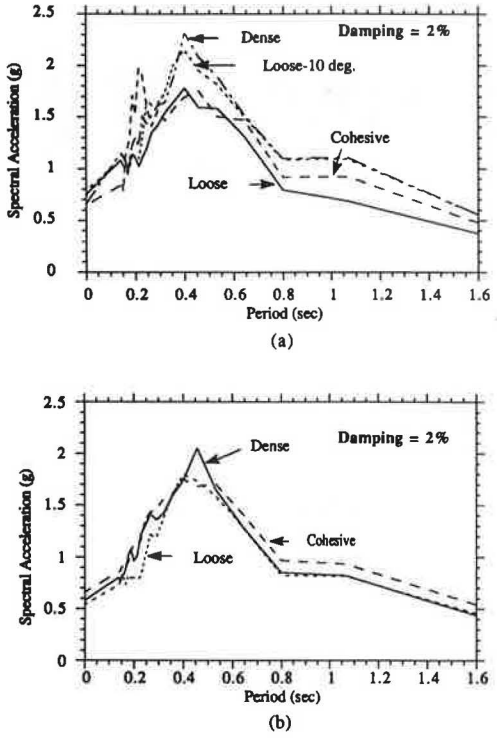

FIGURE 5 Comparison of base acceleration response spectra for a filtered El Centro × 5 for *a*, MSE and *b*, Type 1 models.

DISPLACEMENT BEHAVIOR

Permanent Wall Movement Comparisons

Figure 6a presents displacement time histories at the top of the MSE retaining wall (just below the sound wall) for all four backfill conditions for the filtered El Centro × 5 base motion. Plotted below these motions is the corresponding time history of accelerations at the base of the model for the dense model. The base acceleration time history input motions to the other three models were very similar, as evidenced by the acceleration response spectra in Figure 5a. The first large acceleration pulse of approximately 0.6 *g* produced a significant permanent displacement at the top of the retaining wall for each of the models. The loose model continued to move out significantly during the first 6 sec compared with the other three models. The 10-degree sloping reinforcement reduced the total permanent displacement by a factor of almost four compared with the horizontally placed reinforcement. The total displacements of the cohesive and dense models were also significantly reduced compared with the loose model.

Figure 6b presents displacement time histories at the top of the Type 1 retaining wall (just below the sound wall) for the three different backfill types (loose, dense, and cohesive) during a large comparable filtered El Centro event. Plotted below these motions is the time history of base acceleration for the model with dense backfill. The final permanent displacement of the dense backfill was 50 to 60 percent of the final permanent displacement of the cohesive backfill. The loose backfill displacement was typically 60 to 70 percent of the displacement of the cohesive backfill.

From Figure 6 it is clear that permanent displacements of the Type 1 system are generally smaller than those for the MSE system. For the loose backfill, the permanent displacement at the top of the MSE wall was four times greater than the permanent displacement at the top of the Type 1 wall. For the dense backfill, the permanent displacement at the top of the MSE wall was three times that of the Type 1 wall. With cohesive backfill, however, permanent displacements were similar for both types of walls.

Displacement Mechanisms of Type 1 and MSE Systems with Sound Walls

Figure 7 plots the sequence of incremental permanent displacements at three positions over the height of the wall (LPT1, LVDT2, and LVDT1 in Figure 2a, and LPT2, LVDT2, and LVDT1 in Figure 2b) for the loose models subjected to San

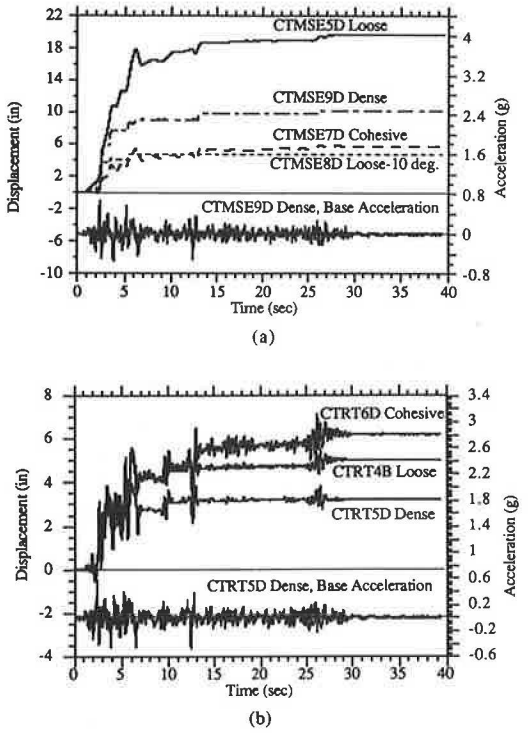

FIGURE 6 Top of retaining wall displacements during a filtered El Centro × 5 event for *a*, four MSE and *b*, three Type 1 models.

Fernando × 4. In all cases the line connecting the top two points should be straight, reflecting the absence of inelastic behavior in the model sound walls. The line connecting the bottom two points should be curved.

The permanent incremental displacements at the top of the sound wall for the MSE models shown in Figure 7a are closely tied to the soil-pile interaction. For the loose and dense models, pile slippage is followed by the sand filling the vacated space and the pile tips not returning to the original position. This results in accumulated rotation of the sound wall. For the cohesion models, enlarged holes generally allowed the sound wall to rotate back near its original position. The curvature of the face of the MSE wall should be concave to the right, consistent with a shear deformation mode of the soil. Further discussion of MSE displacement mechanism is given by Casey et al. (*13*).

For the Type 1 model the permanent incremental displacement of the top of the sound wall in Figure 8b was greater than the top of retaining wall displacement, and one can observe a continuing rotation of the Type 1 wall. The actual displaced shape and the Type 1 retaining wall below the sound wall should curve such that slope compatibility is matched at the retaining wall–sound wall connection. This curvature would therefore always be concave to the left in the figures and create a curvature consistent with the final induced residual moments.

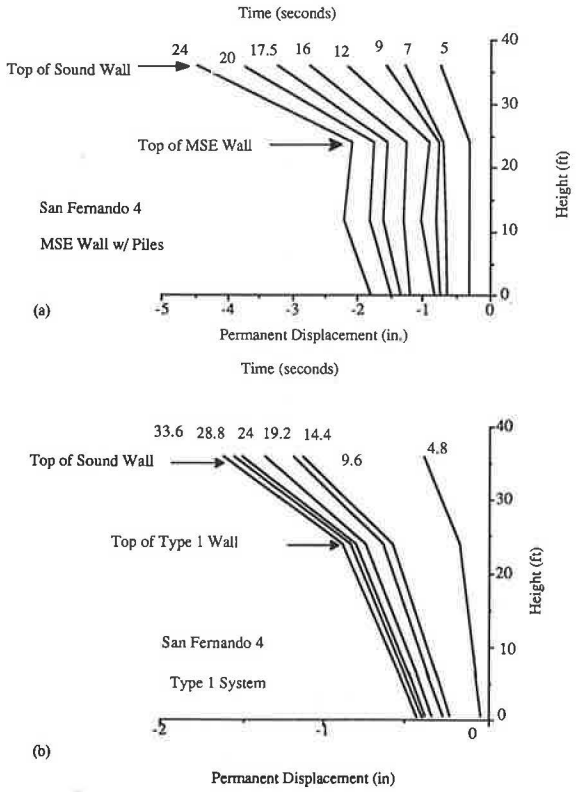

FIGURE 7 Permanent displacement profiles during a San Fernando × 4 event for the loose *a*, MSE and *b*, Type 1 models.

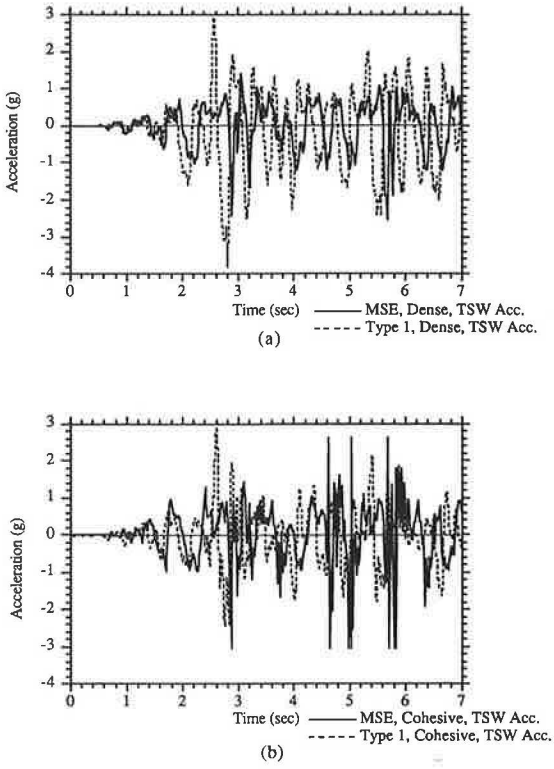

FIGURE 8 Top of sound wall accelerations for the *a*, dense and *b*, cohesive Type 1 and MSE models due to filtered El Centro × 5.

EXPERIMENTALLY DETERMINED YIELD ACCELERATIONS

By analyzing the acceleration recorded by ACC4, in the backfill 2 in. behind the face of the retaining structure, it was possible to determine a cutoff acceleration, which appears to be associated with permanent deformation of the retaining structure. This cutoff acceleration did not appear to be exactly constant. Several of the apparent cutoff accelerations were averaged together as described by Casey et al. (*13*). The cutoff accelerations are presumed to be an estimate of the yield acceleration (*5*). The yield acceleration data determined by this method are summarized as follows.

For the MSE system the loose, loose-10°, dense, and cohesive models had yield acceleration ranges of 0.18 to 0.24 g, 0.22 to 0.27 g, 0.26 to 0.33 g, and 0.34 to 0.41 g, respectively. For the Type 1 system the loose, dense, and cohesive models had yield acceleration ranges of 0.22 to 0.36 g, 0.28 to 0.34 g, and 0.27 to 0.35 g. With the exception of one data point from the loose backfill, the Type 1 deduced yield accelerations for all three backfill types ranged from 0.27 to 0.35 g.

SOUND WALL ACCELERATION COMPARISONS

The filtered El Centro × 4 base motion, imposed on each of the models, represents a severe earthquake with base accelerations as high as 0.7 g. During the interval from 1 to 7 sec the base acceleration had peaks up to 0.7 g, and from 7 to 28 sec the measured base acceleration peaks reached 0.15 g. Results from this motion will be compared for all systems.

The acceleration at the top of the sound wall for these two soil retaining systems differed because of the nature of the sound wall attachment to each retaining wall and filtering of the base motion by the wall/backfill systems. The face plates in the MSE system cannot develop shear or moment, hence lateral displacements at the face of the wall are dominated by elastic and permanent shear strains distributed within the reinforced soil mass. The permanent deformations absorb energy and lower the apparent natural frequencies of vibration. For the Type 1 system the lateral deformations are influenced by the shear and flexural stiffness of the cantilever retaining wall and sliding along the base.

The sound wall with the Type 1 wall is cast monolithically with the concrete retaining wall and hence acts as an elastic extension of the cantilever wall with a nearly fixed base. Therefore, the accelerations induced at the top of the sound wall result in elastic amplifications of the transverse and rotational accelerations at the top of the Type 1 retaining wall accompanied by relatively low damping.

The response of the MSE sound wall, slab, and piles (sound wall system) depends highly on the soil-pile interaction. In the dense and loose models the pile skin friction was exceeded and the piles began to pull out when the effective inertial force acting on the sound wall away from the backfill reached a critical level. At the top of the sound wall this phenomenon was shown to result in a capping of the positive acceleration. As the sound wall moves back toward the backfill, the large resistances provided by the pile tip bearing stiffness are reactivated. This sudden change in stiffness induced high-frequency and large-amplitude accelerations at the top of the sound wall. The resulting acceleration record was nonsymmetric. The slippage of the piles helped to dissipate energy.

Figure 8a presents 7 sec of the top of sound wall acceleration time histories due to filtered El Centro × 5 for the dense models of both the MSE and Type 1 systems. The lack of symmetry on the positive and negative sides is evident for both systems. The positive accelerations for the MSE system are clearly capped at less than 1 g, and several time intervals show extended positive excursions (which will contribute energy dissipation) where some combination of slipping of the piles and sliding of the MSE wall are occurring. The positive peaks for the Type 1 system show little evidence of capping, and the Type 1 maximum positive acceleration is approximately twice the maximum MSE positive acceleration. Essentially all the negative peaks for both systems are sharp. The maximum negative peaks for the MSE system at approximately 2.8 and 5.7 sec are very high frequency associated with the stiffening described earlier.

A third type of behavior possible with the MSE sound wall system was observed in the cohesive model (Figure 8b). In the cohesive backfill the lateral forces from the piles worked to enlarge the holes that held the piles. Since the material was cohesive, the enlarged holes did not refill, and skin friction was lost after a few large acceleration pulses. In these models the effectiveness of the piles was lost, and the sound wall slab was able to lift up and upon returning the slab struck the backfill soil surface. The impacts caused very high acceleration pulses to travel through the sound wall.

The impacts are clearly seen in Figure 8b, which presents the same top of sound wall acceleration comparisons for the cohesive models as Figure 8a does for the dense models. Very high frequency acceleration amplitudes reach the limit of the recorders on both the positive and negative sides for the MSE system, and the peak amplitudes exceed the acceleration peaks recorded for the Type 1 system. The large accelerations developed at the top of the sound wall due to the impacts may induce large moments at the base of the sound wall. However, even if the high moments exist (no strain gauges were present on the sound wall for the MSE tests), the accelerations are of such short duration that they do not result in high velocities or high displacements. The velocity spectrum of the cohesive model was not significantly higher than that of the dense or loose-10° models.

Figures 9a and 9b present the amplifications of the acceleration spectra for the MSE and Type 1 systems from the base of the retaining wall to the top of the sound wall. Excepting the cohesive model, the maximum amplifications for the MSE system in the range of interest (period less than 0.4 sec) are about 5. The larger amplification for the cohesive model may be associated primarily with lift-off and impact of the slab. The amplifications for the Type 1 system are generally much greater than for the MSE system.

The amplification was also calculated for each earthquake by dividing the peak top of sound wall acceleration by the peak base motion. Figure 10a shows these amplification factors as a function of the peak base acceleration. For each earthquake there are only two data points, one for the positive and one for the negative peaks of the base and sound wall accelerations. The amplification does not appear to be a strong function of the base motion, hence a horizontal line is drawn

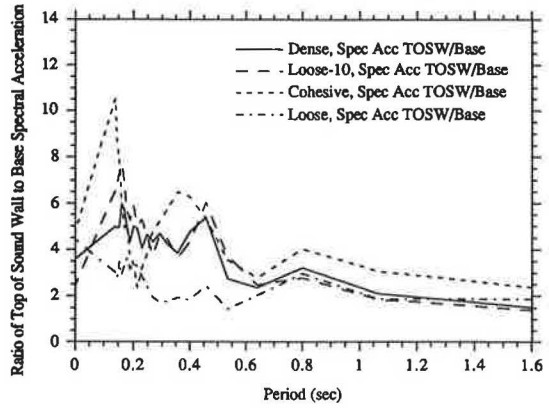

(a)

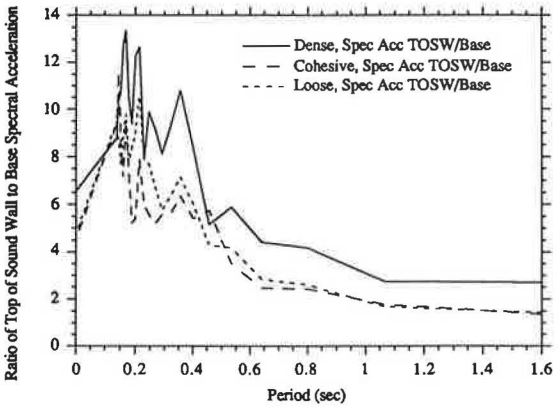

(b)

FIGURE 9 Amplification of spectral acceleration from the base to the top of sound wall in the *a*, MSE and *b*, Type 1 models.

in Figure 10a representing the average amplification for each case. The positive amplifications are smaller than the negative amplifications due to the unsymmetrical resistance for both systems. The Type 1 amplifications are 1.8 to 1.9 times larger than the corresponding MSE amplifications.

Finally, the ratios of Type 1 to MSE top of sound wall acceleration spectra are presented in Figure 10b for the dense, cohesive, and loose models. In general, the Type 1 spectra amplitudes are 1.5 to 3 times greater than the MSE spectral amplitudes over the period range of interest (0.2 to 0.4 sec).

CONCLUSIONS

1. Sound walls superimposed on the Type 1 walls experienced maximum accelerations approximately twice as large as those experienced by sound walls superimposed on MSE systems. This was primarily caused by the monolithic connection between the Type 1 wall and the sound wall and the lower amount of energy dissipated by the backfill behind a Type 1 system.
2. Permanent displacements of MSE walls with sand backfills were clearly related to the competence of the backfill and the amplitude and number of acceleration pulses exceeding the yield acceleration. Displacements at the top of the MSE retaining wall after a large event were three to four times larger than those included at the top of Type 1 walls. Cohesive backfill models did not follow the same trends as the two sand models.
3. The sound wall–slab system with the MSE system needs to be physically separated from the top face plate to avoid striking.
4. An improved anchor at the rear of the slab should be found in place of the piles to minimize the striking and gradual tilting problems.

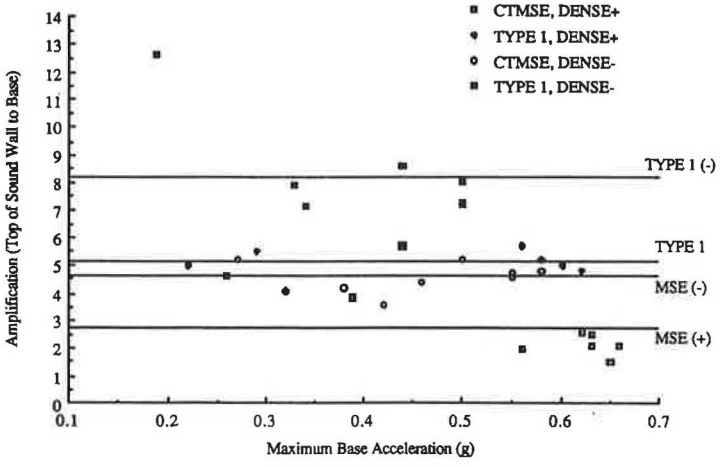

(a)

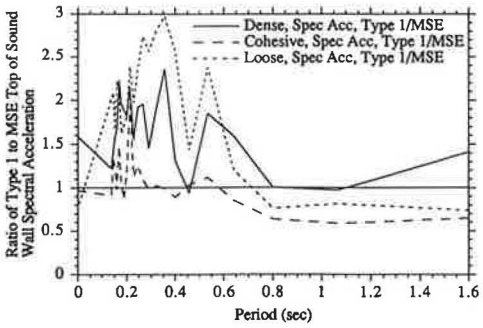

(b)

FIGURE 10 *a*, Amplification of acceleration from base to top of sound wall for all models and all events; *b*, ratio of top of sound wall acceleration spectra, Type 1 divided by MSE, due to filtered El Centro × 5.

ACKNOWLEDGMENTS

This work was carried out with funding from the Federal Highway Administration and Caltrans. The continued review and comments on Ken Jackura are gratefully acknowledged.

REFERENCES

1. N. Mononobe and H. Matsuo. On the Determination of Earth Pressure During Earthquake. *Proc., 2nd World Conference on Earthquake Engineering*, Tokyo, 1929.
2. H. B. Seed and R. V. Whitman. Design on Earth Retaining Structures for Dynamic Loads. *Proc., ASCE Specialty Conference: Lateral Stresses in the Ground*, Cornell University, Ithaca, N.Y., 1970.
3. R. Richards, Jr., and D. G. Elms. Seismic Behavior of Gravity Retaining Walls. *Journal of the Geotechnical Engineering Division*, ASCE, April 1979.
4. N. A. Newmark. Effects of Earthquakes on Dams and Embankments. *Geotechnique*, Vol. 15, 1965.
5. A. Bracegirdle. Seismic Stability of Reinforced Earth Retaining Walls. *Bulletin of the New Zealand National Society for Earthquake Engineering*, 1980.
6. M. D. Bolton and R. S. Steedman. Centrifugal Testing of Microconcrete Retaining Walls Subjected to Base Shaking. *Proc., International Conference of Soil Dynamics and Earthquake Engineering*, Southampton University, England, July 1982.
7. L. A. Ortiz, R. F. Scott, and J. Lee. Dynamic Centrifuge Testing of a Cantilever Retaining Wall. *Earthquake Engineering and Structural Dynamics*, 1983.
8. G. N. Richardson and K. L. Lee. Seismic Design of Reinforced Earth Walls. *Journal of the Geotechnical Engineering Division*, ASCE, Feb. 1975.
9. R. B. Nagel. *Seismic Behavior of Reinforced Earth Wall.* Master of Engineering report. University of Canterbury, Christchurch, New Zealand, 1985.
10. W. E. Wolfe and D. Rea. *Earthquake Induced Deformations in Reinforced Earth Walls*. Mechanics and Structures Department, School of Engineering and Applied Science, University of California, Los Angeles, May 1990.
11. G. N. Richardson. Earthquake Resistant Reinforced Earth Walls. *Proc., ASCE Symposium on Earth Reinforcement*, Pittsburgh, Pa., 1978.
12. B. L. Kutter, J. A. Casey, and K. M. Romstad. Centrifuge Modeling and Field Observations of Dynamic Behavior of Reinforced Soil and Concrete Cantilever Retaining Walls. *Proc., 4th U.S. National Conference on Earthquake Engineering*, Vol. 3, EERI, May 20–24, 1990, Palm Springs, Calif., pp. 663–672.
13. J. A. Casey, D. Soon, B. L. Kutter, and K. M. Romstad. Modeling of Mechanically Stabilized Earth Systems: A Seismic Centrifuge Study. *Proc., ASCE Geotechnical Engineering Congress*, Geotechnical Special Publication 27, Vol. 2, Boulder, Colo., June 1991, pp. 839–850.
14. G. S. Chang. *Centrifugal and Numerical Modeling of Soil-Pile-Structure Interaction due to Seismic Activity*. Ph.D. dissertation. University of California, Davis, 1991.

Publication of this paper sponsored by Committee on Transportation Earthworks.